Title

Tumor-targeting multifunctional micelles for imaging and chemotherapy of advanced bladder cancer

Journal

Nanomedicine, 8(8)

ISSN

1743-5889

Authors

Lin, Tzu-yin

Li, Yuan-Pei

Zhang, Hongyong

et al.

Publication Date

2013-08-01

DOI

10.2217/nnm.12.150

Peer reviewed

Published in final edited form as:
Nanomedicine (Lond). 2013 August ; 8(8): 1239–1251. doi:10.2217/nnm.12.150.

Tumor-targeting multifunctional micelles for imaging and chemotherapy of advanced bladder cancer

Tzu-yin Lin[1], **Yuan-Pei Li**[2], **Hongyong Zhang**[1], **Juntao Luo**[3], **Neal Goodwin**[4], **Tingjuan Gao**[5], **Ralph de Vere White**[6], **Kit S Lam**[1,2], and **Chong-Xian Pan**[*,1,6,7]

[1]Division of Hematology & Oncology, Department of Internal Medicine, School of Medicine, University of California-Davis, Sacramento, CA 95817, USA

[2]Department of Biochemistry & Molecular Medicine, School of Medicine, University of California-Davis, Sacramento, CA 95817, USA

[3]Department of Pharmacology, State University of New York Upstate Medical University, Syracuse, NY 13210, USA

[4]Jackson Laboratory, 4910 Raley Boulevard, Sacramento, CA 95838, USA

[5]NSF Center for Biophotonics Science & Technology, University of California-Davis, Sacramento, CA 95817, USA

[6]Department of Urology, University of California-Davis Cancer Center, Sacramento, CA 95817, USA

[7]Veteran Administration Northern California Health Care System, 10535 Hospital Way, Mather, CA 95655, USA

Abstract

Aim—This work aimed to determine if the treatment outcomes of bladder cancer could be improved by targeting micelles that are decorated with bladder cancer-specific ligands on the surface and loaded with the chemotherapeutic drug paclitaxel.

Materials & methods—Targeting efficacy and specificity was determined with cell lines. An *in vivo* targeting and anti-tumor efficacy study was conducted in mice carrying patient-derived xenografts.

Results & discussion—Targeting micelles were more efficient than nontargeting micelles in delivering the drug load into bladder cancer cells both *in vitro* and *in vivo* ($p < 0.05$). The micelle formulation of paclitaxel was less toxic than free paclitaxel in Cremophor® (Sigma, MO, USA) and allowed administration of three-times the maximum tolerated dose without increasing the toxicity. Targeting micelles were more effective than the nontargeting micelles in controlling cancer growth ($p = 0.0002$) and prolonging overall survival ($p = 0.002$).

*Author for correspondence: Tel.: +1 916 734 3771 Fax: +1 916 734 7946 cxpan@ucdavis.edu.

Financial & competing interests disclosure The authors have no other relevant affiliations or financial involvement with any organization or entity with a financial interest in or financial conflict with the subject matter or materials discussed in the manuscript apart from those disclosed.

Ethical conduct of research The authors state that they have obtained appropriate institutional review board approval or have followed the principles outlined in the Declaration of Helsinki for all human or animal experimental investigations. In addition, for investigations involving human subjects, informed consent has been obtained from the participants involved.

Conclusion—Targeting micelles loaded with paclitaxel offer strong potential for clinical applications in treating bladder cancer.

Keywords

bladder cancer-specific ligand; bladder urothelial carcinoma; diagnostic imaging; nanoparticle; targeted therapy

Human bladder cancer is the fourth most common cancer in males and eighth most common in females [1]. Advanced bladder cancer accounts for the vast majority of deaths due to this disease. Even with significant advances in cancer research, the 5-year mortality rate ranges from 33 to 73% for locally invasive bladder cancer and is less than 10% for metastatic diseases. It has not changed over the last three decades [2]. Therefore, more effective therapeutic agents are greatly needed.

Several nanocarriers have been developed that can deliver chemotherapeutic drugs, DNA [3], RNA [4], and other therapeutic and imaging agents [5–7] with promising results in preclinical bladder cancer studies. Pegylated liposomal doxorubicin has shown significant anticancer activity in a Phase II clinical trial focusing on locally advanced and metastatic bladder carcinoma [8]. The favorable efficacy of nanoparticles mainly depends on the passive enhanced permeability and retention effect secondary to increased microvascular leakage at the tumor sites [9,10]. To further improve the targeting effects of nanoparticles, cancer-targeting ligands have been combined with nanotherapeutics to facilitate the delivery of nanoparticles to cancer sites [11,12] and induce transport of nanoparticles into cancer cells [13–15].

In this article, the authors report on the combination of a bladder cancer-specific ligand named PLZ4 and the micelle drug-delivery system for imaging and therapeutic applications in bladder cancer. PLZ4 (amino acid sequence: cQDGRMGFc – upper case letters represent $_{L}$-amino acids and lower case letters represent unnatural $_{D}$-cysteines used to cyclize and stabilize the peptide) is the first bladder cancer-specific ligand to be identified, and has been shown to target this cancer in both humans and dogs [16,17]. Like other ligands containing the DGR motif, PLZ4 binds to K562 cells expressing $\alpha_v\beta_3$ integrin, but not the parent K562 cell line or K562 cell lines expressing other integrins, suggesting that the target molecule is $\alpha_v\beta_3$ integrin. In addition to DGR, the GF motif is also critical for cell binding and may determine the binding specificity [16]. The self-assembling micelles are composed of a class of linear polyethylene glycol (PEG) and dendritic octamers of cholic acid block copolymers (telodendrimers) [18]. Upon assembly, the cholic acid component of the telodendrimer forms a core that allows the loading of hydrophobic drugs, while the PEG on the exposed surface makes micelles `stealthy' *in vivo* after intravenous administration. The authors have previously synthesized and characterized micelles that are decorated with PLZ4 on the surface for cancer-specific targeted drug delivery (Supplementary Figure 1a; see online at www.futuremedicine.com/doi/suppl/10.2217/NNM.12.150) [19]. The resulting bladder cancer-targeting micelles have a small size of less than 20 nm in diameter, with narrow polydispersity. These targeting micelles selectively deliver imaging and therapeutic drugs to bladder cancer cells. The authors have successfully loaded the PLZ4-micelles with paclitaxel (PTX), a chemotherapeutic agent commonly used in several cancer types including bladder cancer [17]. For clinical use, owing to its poor solubility, PTX is formulated in Cremophor® (Sigma, MO, USA) EL (polyoxyethylated castor oil/ethanol), which is associated with severe allergic reactions in patients [20]. Here, the authors demonstrate that formulation of PTX in micelles could significantly increase the efficacy and decrease the toxicity, allowing administration of high-dose PTX (two- to three-times the maximum tolerated dose [MTD]). The authors hypothesize that multifunctional PLZ4-

micelles can improve the treatment outcomes of bladder cancer through the following three mechanisms: enhanced drug delivery to cancer sites, capacity to administer high-dose PTX and decreased toxicity.

Materials & methods

Synthesis of PLZ4 & micelles, & loading of imaging agents & chemotherapeutic drugs in micelles

Both PLZ4 and telodendrimers were synthesized and characterized (chemical structure, purity and cholic acid conjugation) as previously described (Supplementary Figure 1) [16,18,21]. In brief, dendritic octamers of cholic acid were conjugated onto linear PEG via solution-phase condensation reactions. To synthesize targeting micelles in which 50% of telodendrimers were conjugated to PLZ4, an aqueous-phase `click chemistry' catalyzed by cuprous ion was used to couple the alkyne group on PLZ4 peptides to the azide group at the end of PEG on telodendrimers at a molar ratio of 1:2 (PLZ4:PEG) [22]. After conjugation, no PLZ4 was detected, suggesting that PLZ4 had been successfully conjugated to the telodendrimer. The conjugation was further confirmed with proton nuclear magnetic resonance.

To load PTX or fluorescent dye DiD (Invitrogen, CA, USA) into micelles, PTX/DiD and telodendrimer (20 mg) were dissolved in chloroform (5 ml) in a 10-ml flask. Chloroform was removed on a rota-evaporator under vacuum. Next, 1 ml of normal saline (US Pharmacopeia, Rockville, MA) was added and the mixture was vortexed and sonicated for 30 min at room temperature. The final product was analyzed for drug-loading capacity using HPLC and for micelle size and dispersion using a dynamic light-scattering particle sizer and transmission electron microscopy. The final product was sterilized using a filter (0.22 μm) and stored at 4°C for further studies. The loading capacity was 5–10 mg/ml for PTX in 20 mg/ml of telodendrimer. To synthesize targeting micelles, PLZ4-conjugated telodendrimers were used. After self-assembly, the more hydrophilic PLZ4 ligands were displayed on the surface of micelles.

Cell lines & cell culture condition

Human cancer cell lines were purchased from American Type Culture Collection (ATCC; Manassas, VA, USA) and maintained with the recommended medium. The human bladder cancer cell line 5637 was further transfected with a green fluorescent protein for *in vitro* and *in vivo* monitoring. The 5637 cell line was purchased from ATCC in 2009 and was authenticated by ATCC with microsatellite analysis in 2011. The dog bladder cancer cell line K9TCC-Pu-In was originally developed and directly provided by Deborah Knapp at Purdue University (IN, USA) in July 2009. These cell lines were tested and authenticated using the morphology, immunohistochemistry, gene expression and tumorigenicity assays in Knapp's laboratory in 2009. As these cells were obtained directly from Knapp, who performed cell line characterizations, and passaged in the user's laboratory for less than 6 months after resuscitation, reauthorization was not required.

Affinitofluorescence

Touch preparation slides were obtained from clinical bladder cancer specimens after cystectomy or transurethral resection. This study was approved by the University California-Davis Institutional Review Board with informed consent obtained before the procedure. Samples were fixed with acetone for 2 min and stored at 4°C before testing. As previously described, samples were incubated with 5 μM of biotinylated PLZ4 in 0.05% Tween®20 (Sigma)/phosphate-buffered saline (PBS) for 1 h at room temperature. After washing three times, streptavidin-Alex488® (Invitrogen) was applied to the slides for another 1 h. 4′,6-

diamidino-2-phenylindole-containing solution (Sigma) was used for nuclear staining after washing to remove unbound streptavidin-Alex488. Imaging was acquired and analyzed by the Metamorph® imaging system (Molecular Devices, CA, USA).

High-resolution topography

To clearly visualize the uptake and distribution of micelles at the subcellular level, green fluorescent protein-expressing 5637 cells were cultured on a glass bottom culture dish (MatTek Corp., MA, USA) overnight. Micelles were diluted to 0.5-μg/ml telodendrimers in the complete culture medium and incubated with cells for 1 h. After lightly washing three times to remove unbound micelles, cells were fixed with 10% formalin for 20 min and mounted with 4′,6-diamidino-2-phenylindole medium for nuclear staining. Slides were observed by a DeltaVision® imaging system (Applied Precision, CA, USA) as per the manufacturer's protocol.

Measurement of caspase 3/7 activity

The SensoLyte® Homogeneous Aminomethylcoumarin Caspase-3/7 Assay Kit (AnaSpec, CA, USA) was used to measure the induction of caspase 3/7. Briefly, 5637 cells were seeded in 96-well plates at 20,000 cells per well in 100 μl. Cells were then treated with different concentrations of free PTX, PTX-loaded nontargeting or PTX-loaded targeting micelles, as indicated. After 24 h of incubation, 50 μl of working solution was added, and the mixture was shaken for 40 min. The fluorescence was measured by a microplate reader (Molecular Devices). Wells with medium and working solution served as blanks. This experiment was performed in triplicate and repeated three times.

Establishment of patient-derived xenografts

The animal protocol was approved by the University California-Davis Institutional Animal Care and Use Committee before experiments were performed. To establish subcutaneous patient-derived xenografts (PDXs), 4–5-week-old NOD SCID-γ (NSG; the Jackson Laboratory Bar Harbor, ME, USA) mice were used. Fresh, unmanipulated clinical tumor fragments (3–5 mm^3) were loaded into a trochar with sterile forceps. The loaded trochar was then gently pushed into the flank skin and the trochar plunger was depressed to eject the tumor fragments. The trochar was gently removed and the injection area was sterilized.

To generate an orthotopic xenograft model in NSG mice, a passage 1 PDX specimen was used. BL269 tissue was harvested and cut into small pieces. After treatment with 1 ml of Accutase™ (Innovative Cell Technology, CA, USA) for 30 min at 37°C, single-cell suspensions were obtained after filtering through cell strainers (BD Falcon, CT, USA) to remove larger tissues. Cells in 5–10 μl PBS were then injected into mouse bladder walls, which were visually located under general anesthesia. Mice were monitored every day after surgery.

In vivo xenograft imaging study

Human bladder cancer xenografts were routinely established in the 5–8-week-old nude mice (Harlan, IN, USA). To compare micelle delivery, the human non-small-cell lung cancer cell line H232A was planted at the left lower flank and bladder cancer cell lines or tissues were injected at the right. Three bladder cancer xenografts were established using a human bladder cancer cell line (5637), human clinical bladder cancer specimen (HBC1) and a dog bladder cancer cell line (K9TCC-Pu-In). When the tumor xenografts reached 0.5–1.0 cm, mice were injected with 100 μl of PLZ4-micelles loaded with DiD/PTX and the whole-body imaging was carried out at 0 and 8 h. Mice were then sacrificed. Both tumors and major

organs were harvested for *ex vivo* imaging. Images were processed, quantified and analyzed by Kodak imaging software (Kodak, NY, USA).

Therapeutic efficacy study in a subcutaneous xenograft model in mice

To evaluate the anticancer efficacy and toxicity of PTX-loaded targeting micelles, NSG mice bearing PDXs at the size of 150–200 mm^3 were used with six mice per group. A total of six doses for each treatment group were given intravenously every 3–4 days. Tumor size was measured every 3–4 days and calculated using the formula: 0.5 × length × $width^2$ (mm^3). Bodyweight, appetite, hair coat and activity were monitored regularly. When tumors reached the 1500 mm^3 tumor end point, animals were euthanized for humane reasons. Blood was drawn 2 days after the fourth dose for blood counts, and liver and kidney function tests. Another eight mice were implanted with PDXs at both sides and were then treated with PBS, free PTX 10 mg/kg, nontargeting micelle loaded with PTX, and PLZ4-targeting micelle loaded with PTX, for four doses with a 3-day interval. Mice were sacrificed after the fourth dose and tumors were harvested for histopathological evaluation.

Statistics

The experiments were repeated at least in triplicate. The mean values and standard deviation are presented for each set of experiments. For determination of micelle delivery to tumor sites, the authors calculated mean fluorescence intensities of the tumor area and of the normal tissue area by means of the region-of-interest function using Kodak Image Analysis Software (Kodak), then plotted a pseudocolored scale based on the semiquantitative information from near-infrared fluorescence images by integrating fluorescence intensities from equal areas within tumor and normal tissue regions. The Student *t*-test was used for statistical analysis. p-values of less than 0.05 were considered to be significant.

Results

Characterization of PLZ4-micelles

The loading efficiency is defined as the ratio of drug loaded into micelles to the initial drug content. Owing to the hydrophobic nature of PTX, the loading efficiency was 99.4%, suggesting that almost all of the PTX was incorporated into the hydrophobic core of micelle. The PTX loading capacity was 24.9% (w/w of PTX/PLZ4-telodendrimer). The drug-loading capacity is sufficient for clinical application since the authors have previously shown that telodendrimer at 2 mg/ml was not toxic to cells [21]. The PLZ4 ligand density on the surface was 50%, as the molar ratio of PLZ4 to telodendrimer was 1:2 during the conjugation with `click chemistry', and no free PLZ4 was detected after conjugation. Micelles were stable during the *in vitro* incubation for 4 days in PBS with 10% fetal bovine serum at 37°C (Figures 1B & 1C). To determine the drug release, PLZ4-micelles loaded with PTX were dialyzed against PBS with 10% fetal bovine serum. There was an immediate release of approximately 20% PTX into the dialysate within 5 min, possibly related to equilibrium effect, which stabilized after 5 min. At 24 h, approximately 74% PTX remained in PLZ4-micelles. As the authors previously reported, the authors confirmed the size (approximately 23 nm in diameter) and morphology with transmission electron microscopy [19].

Targeted delivery of PLZ4-micelles & the drug load into bladder cancer cells

Before the authors determined the targeting efficiency of PLZ4-micelles, the authors determined that PLZ4 could bind to fresh bladder cancer cells from clinical specimens (Supplementary Figure 2). To determine if targeting PLZ4-micelles could specifically deliver the drug load to human bladder cancer cells, cells were incubated with different concentrations of DiD in nontargeting or targeting micelles for 30 min before washing to

remove unbound micelles. Targeting micelles decorated with PLZ4 on the surface delivered much more DiD to 5637 cells and another bladder cancer cell line, T24, than the nontargeting micelles (Figure 2A). These results were further validated by the high-resolution topography shown in Figure 2B in 5637 cells treated with nontargeting and targeting micelles both loaded with DiD (6.25 μg/ml, 30-min incubation). Targeting micelles accumulated in the cytoplasm with a multifocal aggregate pattern, while nontargeting micelles accumulated in the cytoplasm to a lesser extent and in a scattered pattern. This increased drug delivery was translated into increased induction of caspase 3/7 (Figure 2C).

Development of PDXs of bladder cancer in NSG mice

Most tumor xenograft models used in laboratory research are derived from cell lines that have been selected, cultured and maintained *in vitro* for a long time. The cell-surface molecules of these cells may be different from primary cancer cells in patients. To address this issue, University California-Davis and the Jackson Laboratory West have collaborated to develop PDXs in NSG mice. These mice lack mature T cells, B cells and high-affinity receptors for several cytokines, such as IL-2, -4, -7, -9, -15 and -21 [23]. Therefore, these mice have defective NK cells and further impaired innate immunity that allows for better engraftment of human cancer tissue. Unselected and unmanipulated clinical cancer specimens were directly injected subcutaneously into mice to establish xenografts. The pathological fidelity was maintained in different passages in mice (Figure 3A). To establish a locally advanced bladder cancer NSG model, the authors injected a single-cell suspension of patient-derived bladder cancer cells directly into the bladder wall. Mice developed patient-derived locally advanced bladder cancer xenografts (corresponding to T2–T4 stages) within a few weeks (Figure 3B).

Selective accumulation of targeting micelles in bladder cancers

In order to compare bladder cancer-targeting specificity while avoiding interanimal variability, the authors assessed two different cancer xenografts in the same mice. At the left flank of each mouse, the authors established a xenograft from H232A lung cancer cells, which PLZ4 does not bind to (Figure 4). At the right flank, the authors established bladder cancer xenografts from: human 5637 cell line (Figure 4A); human bladder cancer 1 (PDX from a clinical patient specimen; Figure 4B); or a dog bladder cancer cell line K9TCC-Pu-In (Figure 4C). Both *in vivo* and *ex vivo* studies detected higher DiD signals at the bladder cancer xenografts than at the H232A xenografts in the same mice. Muscle always has low signal in micelle studies when compared with liver, kidney and lung, as many agents are metabolized/excreted in the liver and kidney, and lung has high blood volume [24–26]. Therefore, the authors normalized the DiD signal in tumor xenografts with the signal in muscle, as previously reported [19]. After normalization, bladder cancers had a significantly higher degree of fluorescence signal than the H232A lung cancer (Figure 4D, $p < 0.05$). This result was in agreement with the microscopic observation that showed stronger near-infrared red fluorescence in the bladder cancer xenografts compared with in lung xenografts (Figure 4E).

More efficacious anti-tumor activity associated with targeting micelles

Next, the authors determined if the enhanced drug delivery can be translated into improved efficacy in cancer control and overall survival. When PDXs reached 150–200 mm^3 in size, mice received one of the following six different treatments (Table 1): PBS, free PTX at 10 mg/kg of bodyweight (the MTD), PTX at 10 mg/kg in the nontargeting (nanomicelle loaded with PTX [NM-PTX]) or targeting (nanomicelle coated with PLZ4 and loaded with PTX [PLZ4-NM-PTX]) micelles, PTX at 30 mg/kg in NM-PTX or PLZ4-NM-PTX. Mice were treated every 3 days for six doses. Tumor sizes were monitored twice a week. As shown in

Figure 5a, these tumor xenografts were highly aggressive. All mice that received PBS reached the end point (mouse death from disease or tumor volume more than 1500 mm^3) before receiving all six treatments. Mice that received 10 mg/kg PTX showed significant inhibition of *in vivo* tumor growth and significantly longer overall survival compared with the control PBS group. However, no significant difference was observed between different formulations of PTX at 10 mg/kg. For mice that received 30 mg/kg NM-PTX or PLZ4-NM-PTX, all tumors responded to the treatment, and achieved durable response when compared with the mice that received PTX at 10 mg/kg ($p < 0.0001$). Tumors regrew approximately 45 days after the first treatment. Prolonged tumor control was translated into prolonged overall survival (Figure 5B). Compared with mice that received 30 mg/kg PTX in nontargeting micelles, mice that received 30 mg/kg PTX in targeting PLZ4-micelles demonstrated a significantly longer time to tumor growth (52.6 vs 58.1 days; $p = 0.0002$), and overall survival (64 vs 76 days; $p = 0.002$). Time to tumor growth is defined as the interval from the time when mice receive treatment to the time that tumor xenografts grow to the pretreatment level. Overall survival is defined as the interval from the time when mice receive treatment to the time when mice die from tumor, toxicity or are euthanized for humane reasons. In conclusion, targeting micelles had better efficacy than nontargeting micelles at a higher dose.

Reduced toxicity associated with micelle formulation of PTX

All mice that received PTX had decreased activity, especially in the group treated with free PTX injection. One mouse in this group died after the sixth dose of free PTX, which may be attributed to accumulated PTX toxicity and/or response toward Cremophor solvent for PTX formulation. Mice started losing weight at comparable extents in all groups, but a little more bodyweight loss was noted after the fourth dose (Figure 5C). However, these mice regained the weight during the fifth and sixth doses, suggesting that the weight loss may not be related to drug toxicity.

On day 13 (after dose 4), blood tests to monitor blood counts and chemistry panels were performed. As expected, mild anemia and marked leukopenia were noted in the mice receiving 10 mg/kg PTX, indicating bone marrow toxicity(table 1). Those changes were significantly more severe in mice that received free PTX than in the mice treated with PTX in the nontargeting or targeting micelle formation at the same dose. At the same dose level of 10 mg/kg, mice that received PTX in the nontargeting or targeting micelles had higher white and red blood cell counts than those mice that received free PTX, suggesting lower toxicity. Interestingly, mice treated with PTX in the micelle formulation at 30 mg/kg (three-times the MTD), had similar levels of white and red blood cell and platelet counts as the mice treated with free PTX at 10 mg/kg, suggesting that micelle formulation may allow administration of high-dose chemotherapy without the associated toxicity. No notable changes in liver and kidney biochemical profiles were observed in any treatment group. In conclusion, both nontargeting and targeting micelle formulations have less bone marrow toxicity than free PTX at the dose of 10 mg/kg, and could safely deliver 30 mg/kg of PTX repeatedly with tolerable toxicity.

As PTX is not water soluble, it is dissolved in Cremophor EL/ethanol, which causes mast cell degranulation and some of the toxicity. The authors cultured mouse bone marrow-derived mast cells, and evaluated the degranulation after treatment with various agents. Mouse bone marrow-derived mast cell degranulation was significantly higher after treatment with PTX in Cremophor EL/ethanol compared with treatment with PTX in Cremophor-free nontargeting or targeting micelles at the same final PTX concentration (Supplementary Figure 3).

Dose-dependent cell-cycle arrest & histopathological analysis

The authors next determined if improved cancer control and decreased toxicity were associated with the underlying histopathological changes. Another group of mice were sacrificed and histopathological examination of tumor and major organs was performed on day 14. PTX stabilizes microtubules and arrests cell cycle at the Gap2/mitosis (G2/M) phase. The authors observed a dose-dependent cell-cycle arrest at the tumor xenografts in the mice treated with targeting micelles (Supplementary Figure 4a). Consistent with low toxicity in other major organs, the authors did not see significant cell-cycle arrest or pathological changes in other major organs, including the rapidly dividing small intestine epithelial cells (Supplementary Figure 4B), suggesting cancer-specific drug delivery and anti-tumor activity.

Discussion

In this article, the authors present a novel multifunctional nanotherapeutics platform that can selectively and efficiently deliver both diagnostic and therapeutic agents to bladder tumors *in vivo*. Our efficacy and toxicity results support its potential to be used for both imaging detection and therapeutic applications for advanced bladder cancer.

Bladder cancer-specific ligand PLZ4 showed strong affinity toward several primary bladder cancers (Supplementary Figure 2) and contributed to the delivery of targeting micelles to the cell surface, which then triggers uptake of whole micelles into cells (Figure 2B). In the PLZ4-micelle, PLZ4 is displayed on the distal terminus of PEG that could be exposed outside or within the PEG corona of the micelle. Even though there is no simple way to determine the actual proportion of PLZ4 displayed outside versus inside of the PEG corona, functional analysis suggests that addition of PLZ4 did enhance the delivery of micelles into bladder cancer cells. As shown in Figure 2, PLZ4-coated micelles delivered a much greater drug load to the target cells compared with micelles without PLZ4. These results suggest that PLZ4 can not only guide the delivery of micelles to bladder cancer cells, but may also be used for guided delivery of other imaging and therapeutic agents, such as toxins or radioisotopes.

Several nanotherapeutics platforms have been developed. Those nanoparticles mainly take advantage of the passive enhanced permeability and retention effect. Our group was the first to developed a bladder cancer-specific ligand, and combine it with our newly developed micelle platform to develop these bladder cancer-specific nanotherapeutics. These targeting PLZ4-micelles mitigate drug toxicity, delay tumor growth and improve overall survival (Figure 5 & table 1). It is interesting to find that at the same dose of 10 mg/kg, PTX in the micelle formulations was no more effective than the free PTX even though they were associated with less toxicity. As nanoparticles can be cleared *in vivo* by reticuloendothelial cells (including the liver) and PTX is normally metabolized by the liver, the dose of 10 mg/kg of PTX in micelles may be subtherapeutic even though it is the MTD for free PTX. At this dose, the authors did not observe any clinical and biochemical toxicity at all, further supporting that the dose of 10 mg/kg of PTX in micelles is subtherapeutic.

These targeting PLZ4-micelles have the potential to be used for imaging detection as they can specifically deliver the drug load to bladder cancer sites. However, the leakage of imaging agents from micelles needs to be addressed. In our previous study, a small amount of DiD accumulated in tumor xenografts or vital organs in the mice that received intravenous free DiD, while PLZ4-micelles loaded with DiD mainly accumulated in tumor xenografts derived from a dog bladder cancer cell line [19]. Premature release of DiD from nanoparticles is certainly present. However, it should not significantly affect the imaging result as they will be rapidly metabolized. To address the premature release of DiD dye or

drugs, the authors have recently developed crosslinked micelles that can release the drug load at the tumor site [26].

Nanoformulation of chemotherapeutic drugs decreases the toxicity. The dose of PTX dissolved in Cremophor EL and dehydrated alcohol (Taxol®, Bristol-Myers Squibb, NY, USA) is usually approximately 175 mg/m^2 of body surface area via intravenous injection every 3 weeks. When it is nanoformulated with albumin (Abraxane®, Celgene, NJ, USA), the dose increases to 260 mg/m^2 via intravenous injection every 3 weeks. Similar findings were also observed with doxorubicin, a medication also effective in bladder cancer as part of the MVAC regimen (including methotrexate, vinblastine, doxorubicin and cisplatin). The lifetime cumulative dose of free doxorubicin is usually less than 450 mg/m^2 secondary to its cardiac toxicity. However, the liposomal formulation of doxorubicin significantly decreases the toxicity and allows administration of doxorubicin at much higher doses than that allowed for free doxorubicin [27–29]. Similar findings were also observed in the authors' study. While the MTD for PTX was approximately 10 mg/kg for repeated dosing [30], the authors were able to deliver 30 mg/kg PTX in micelles with limited toxicity and zero mortality (table 1). Moreover, the authors further provided *in vitro* evidence that the micelle formulation of PTX was less likely to induce mast-cell degranulation than the Cremophor EL-based PTX (Supplementary Figure 3). In addition, PEG is part of the micelle structure that is displayed on the surface and makes micelle `stealthy'. This is consistent with the authors' previous findings that PLZ4-micelles favorably concentrated at dog bladder cancer xenografts, but little in other organs, since PLZ4 specifically binds to bladder cancer cells [19]. This may explain the findings that cell-cycle arrest was observed in tumor xenografts but was not seen in other major organs in the mice when they were treated with targeting micelles loaded with PTX (Supplementary Figure 4). Owing to the decreased toxicity, nanoformulations facilitate the administration of high-dose chemotherapy, which can improve cancer control and overall survival (Figure 5).

Compared with many other nanoparticles, the micelles used in this study have small sizes that can be further tuned to different sizes if needed. The small size of our micelle system could increase drug delivery to cancer sites and decrease the nonspecific delivery to other organs, which may contribute to decreased toxicity. Some of our coauthors (Li Y, Lao J and Lam K) showed that, when compared with micelles at 154 nm, micelles with diameters of 17 and 64 nm had higher drug delivery to cancer xenografts and less nonspecific delivery to other organs [18]. In contrast to Abraxane (130 nm in diameter) and Doxil® (Johnson & Johnson, NJ, USA; 90 nm), our targeting PLZ4-micelles have a diameter of approximately 20 nm.

In addition to the small size, cancer-targeting ligands can further increase drug delivery and enhance the anticancer activity of PLZ4-micelles. Several studies have already demonstrated that conjugation of cancer-targeting ligands can guide and increase the delivery of nanoparticles to cancer cell surfaces, or transport nanoparticles into target cancer cells. PLZ4 possesses both properties and significantly increases drug delivery (Figure 2), which the authors demonstrated is translated into improved cancer control and overall survival compared with nontargeting micelles at the same dose (Figure 5). The authors did not observe improved tumor control at low dose. This may be secondary to the high aggressiveness of the cancer that masks the small difference at that dose level. In addition, micelle formulation can change drug release and modulate its cytotoxic effects. Therefore, 10 mg/kg may be the MTD for free PTX, but subtherapeutic for PTX in the micelle formulation.

This is the first report discussing the efficacy and toxicity of nanoparticles in mice carrying xenografts directly developed from unselected and unmanipulated primary tumor specimens

from patients. Most other studies involving nanoparticles use cell lines to generate tumor xenografts. Cell lines have been selected and maintained *in vitro* for a long time, and probably express proteins on their cell surface that may be very different from those in primary clinical cancer. The authors used patient clinical bladder cancer specimens, minced into small pieces and directly injected into NSG mice to establish these xenografts. These patient-derived xenografts maintain structural fidelity (Figure 3a). The results with this model may be more applicable in the clinical setting.

Conclusion

The authors successfully developed a novel targeting micelle-based nanocarrier system against advanced bladder cancers. Taking advantage of micelle formulation, cancer-targeting micelles can not only improve cancer control, but also decrease bone marrow toxicity, enhance drug tolerance and mitigate allergic reaction to PTX in Cremophor. The bladder cancer-specific peptide PLZ4 further elevated the cellular uptake, homing efficiency, cancer selectivity and anticancer efficacy compared with nontargeting micelles. Taken together, these bladder cancer-targeting nanocarriers can potentially improve the treatment outcomes of advanced bladder cancers.

Future perspective

The prognosis for advanced bladder cancer has not changed over the last three decades. Nonspecific cytotoxic chemotherapeutic agents are still the main treatment. However, they are associated with significant toxicity and moderate efficacy in bladder cancer. Targeted therapy is widely used in many other cancer types but not in bladder cancer. A bladder cancer-targeting ligand has recently been developed that can be conjugated to imaging and therapeutic agents for diagnosis, imaging detection and targeted therapy against bladder cancer. The authors expect to see more clinical trials for targeted therapy in bladder cancer within the next 5 years. Nanoformulation of therapeutic agents has been used in the clinical setting to decrease therapy-related toxicity and possibly improve efficacy. The combination of nanomedicine with cancer-targeting ligands has been shown to further increase the anticancer efficacy. For the PLZ4-micelles loaded with PTX, pharmacology and toxicology studies are currently in progress. A Phase I clinical trial has been proposed to study pharmacokinetics, drug delivery to tumor sites, efficacy and toxicity in dog patients with spontaneous bladder cancer. As the active drug of this formulation is PTX, which is widely used in bladder cancer with moderate effect, the nanoformulation can potentially decrease the toxicity, improve the efficacy and possibly gain US FDA approval within the next 5–10 years. More clinical trials with other nanoformulations and nanotherapeutics will also be open in the next few years.

Supplementary Material

Refer to Web version on PubMed Central for supplementary material.

Acknowledgments

Special thanks to P Henderson for insightful comments on experimental design; K Xiao, Y-J Wang for the comments and assistance with experiments; M Bradnam for editing and critical comments during manuscript preparation; R Gandour-Edwards for coordinating the specimen collection and the establishment of patient-derived xenografts between University California-Davis (CA, USA) and Jackson Laboratory West (CA, USA), and C Morh at University California-Davis School of Veterinary Medicine (CA, USA) for pathology interpretation.

This study was supported by the Veteran Administration Career Development Award-2 (Principal Investigator: C-X Pan) and the National Cancer Institute Cancer Center Support Grant (Principal Investigator: R de Vere White) and

Cancer Clinical Investigator Team Leadership Award (C-X Pan). Lamnotherapeutics founded by K Lam and J Luo, is in the process of developing nanomicelles for medical applications and possibly commercializing the product.

No writing assistance was utilized in the production of this manuscript.

References

1. Kirkali Z, Chan T, Manoharan M, et al. Bladder cancer: epidemiology, staging and grading, and diagnosis. Urology. 2005; 66:4–34. [PubMed: 16399414]
2. Herr HW, Dotan Z, Donat SM, Bajorin DF. Defining optimal therapy for muscle invasive bladder cancer. J. Urol. 2007; 177:437–443. [PubMed: 17222605]
3. Matsumoto K, Kikuchi E, Horinaga M, et al. Intravesical interleukin-15 gene therapy in an orthotopic bladder cancer model. Hum. Gene Ther. 2011; 22:1423–1432. [PubMed: 21554107]
4. Seth S, Matsui Y, Fosnaugh K, et al. RNAi-based therapeutics targeting survivin and PLK1 for treatment of bladder cancer. Mol. Ther. 2011; 19:928–935. [PubMed: 21364537]
5. Chihara Y, Fujimoto K, Kondo H, et al. Anti-tumor effects of liposome-encapsulated titanium dioxide in nude mice. Pathobiology. 2007; 74:353–358. [PubMed: 18087200]
6. Cho EJ, Yang J, Mohamedali KA, et al. Sensitive angiogenesis imaging of orthotopic bladder tumors in mice using a selective magnetic resonance imaging contrast agent containing VEGF121/rGel. Invest. Radiol. 2011; 46:441–449. [PubMed: 21512397]
7. Lu Z, Yeh TK, Tsai M, Au JL, Wientjes MG. Paclitaxel-loaded gelatin nanoparticles for intravesical bladder cancer therapy. Clin. Cancer Res. 2004; 10:7677–7684. [PubMed: 15570001]
8. Winquist E, Ernst DS, Jonker D, et al. Phase II trial of pegylated-liposomal doxorubicin in the treatment of locally advanced unresectable or metastatic transitional cell carcinoma of the urothelial tract. Eur. J. Cancer. 2003; 39:1866–1871. [PubMed: 12932664]
9. Matsumura Y, Maeda H. A new concept for macromolecular therapeutics in cancer chemotherapy: mechanism of tumoritropic accumulation of proteins and the antitumor agent smancs. Cancer Res. 1986; 46:6387–6392. [PubMed: 2946403]
10. Maeda H. The enhanced permeability and retention (EPR) effect in tumor vasculature: the key role of tumor-selective macromolecular drug targeting. Adv. Enzyme Regul. 2001; 41:189–207. [PubMed: 11384745]
11. Wu AM, Yazaki PJ, Tsai S, et al. High-resolution microPET imaging of carcinoembryonic antigen-positive xenografts by using a copper-64-labeled engineered antibody fragment. Proc. Natl Acad. Sci. USA. 2000; 97:8495–8500. [PubMed: 10880576]
12. Yang L, Peng XH, Wang YA, et al. Receptor-targeted nanoparticles for *in vivo* imaging of breast cancer. Clin. Cancer Res. 2009; 15:4722–4732. [PubMed: 19584158]
13. Hussain S, Pluckthun A, Allen TM, Zangemeister-Wittke U. Antitumor activity of an epithelial cell adhesion molecule targeted nanovesicular drug delivery system. Mol. Cancer Ther. 2007; 6:3019–3027. [PubMed: 18025286]
14. Kirpotin DB, Drummond DC, Shao Y, et al. Antibody targeting of long-circulating lipidic nanoparticles does not increase tumor localization but does increase internalization in animal models. Cancer Res. 2006; 66:6732–6740. [PubMed: 16818648]
15. Pun SH, Tack F, Bellocq NC, et al. Targeted delivery of RNA-cleaving DNA enzyme (DNAzyme) to tumor tissue by transferrinmodified, cyclodextrin-based particles. Cancer Biol. Ther. 2004; 3:641–650. [PubMed: 15136766]
16. Zhang H, Aina OH, Lam KS, et al. Identification of a bladder cancer-specific ligand using a combinatorial chemistry approach. Urol. Oncol. 2012; 30(5):635–645. [PubMed: 20888272]
17. Lin TY, Zhang H, Wang S, et al. Targeting canine bladder transitional cell carcinoma with a human bladder cancer-specific ligand. Mol. Cancer. 2011; 10(1):9. [PubMed: 21272294]
18. Luo J, Xiao K, Li Y, et al. Well-defined, size-tunable, multifunctional micelles for efficient paclitaxel delivery for cancer treatment. Bioconjug. Chem. 2010; 21:1216–1224. [PubMed: 20536174]
19. Lin, T-y; Zhang, H.; Luo, J., et al. Multifunctional targeting micelle nanocarriers with both imaging and therapeutic potential for bladder cancer. Int. J. Nanomed. 2012; 7:2793–2804.

20. Gelderblom H, Verweij J, Nooter K, Sparreboom A. Cremophor EL. The drawbacks and advantages of vehicle selection for drug formulation. Eur. J. Cancer. 2001; 37:1590–1598. [PubMed: 11527683]
21. Xiao K, Luo J, Fowler WL, et al. A self-assembling nanoparticle for paclitaxel delivery in ovarian cancer. Biomaterials. 2009; 30:6006–6016. [PubMed: 19660809]
22. Tornoe CW, Christensen C, Meldal M. Peptidotriazoles on solid phase: [1,2,3]-triazoles by regiospecific copper(i)-catalyzed 1,3-dipolar cycloadditions of terminal alkynes to azides. J. Org. Chem. 2002; 67:3057–3064. [PubMed: 11975567]
23. Shultz LD, Lyons BL, Burzenski LM, et al. Human lymphoid and myeloid cell development in NOD/LtSz-SCID IL2R gamma null mice engrafted with mobilized human hemopoietic stem cells. J. Immunol. 2005; 174:6477–6489. [PubMed: 15879151]
24. Kato J, Li Y, Xiao K, et al. Disulfide cross-linked micelles for the targeted delivery of vincristine to B-cell lymphoma. Mol. Pharm. 2012; 4(9):1727–1735. [PubMed: 22530955]
25. Xiao K, Li Y, Lee JS, et al. `OA02' peptide facilitates the precise targeting of paclitaxel-loaded micellar nanoparticles to ovarian cancer *in vivo*. Cancer Res. 2012; 72:2100–2110. [PubMed: 22396491]
26. Li Y, Xiao W, Xiao K, et al. Well-defined, reversible boronate crosslinked nanocarriers for targeted drug delivery in response to acidic pH values and *cis*-diols. Angew. Chem. Int. Ed. Engl. 2012; 51(12):2864–2869. [PubMed: 22253091]
27. Grenader T, Goldberg A, Gabizon A. Monitoring long-term treatment with pegylated liposomal doxorubicin: how important is intensive cardiac follow-up? Anti-Cancer Drugs. 2010; 21:868–871. [PubMed: 20679886]
28. Theodoulou M, Hudis C. Cardiac profiles of liposomal anthracyclines: greater cardiac safety versus conventional doxorubicin? Cancer. 2004; 100:2052–2063. [PubMed: 15139046]
29. Kesterson JP, Odunsi K, Lele S. High cumulative doses of pegylated liposomal doxorubicin are not associated with cardiac toxicity in patients with gynecologic malignancies. Chemotherapy. 2010; 56:108–111. [PubMed: 20407236]
30. Sparreboom A, van Tellingen O, Nooijen WJ, Beijnen JH. Nonlinear pharmacokinetics of paclitaxel in mice results from the pharmaceutical vehicle Cremophor EL. Cancer Res. 1996; 56:2112–2115. [PubMed: 8616858]

Executive summary

PLZ4 bladder cancer-targeting ligand

- The bladder cancer-specific ligand PLZ4 can bind to bladder cancer cells from clinical patient specimens.

Characterization of PLZ4-micelles

- PLZ4-micelles have a size of approximately 23 nm in diameter and are stable during the 4-day incubation.

Drug delivery with cell lines

- Targeting micelles decorated with PLZ4 on the surface can not only attach to bladder cancer cell surfaces but, more importantly, transport the whole micelles together with the drug load into target cells.
- Targeting micelles are more efficient in drug delivery to bladder cancer cells than nontargeting cells.

Patient-derived xenografts

- Subcutaneous and orthotopic patient-derived xenografts are developed from unselected and unmanipulated clinical bladder cancer specimens that can be useful in research for bladder cancer.
- The pathological fidelity of patient-derived xenografts is maintained during passaging in mice.

***In vivo* studies of PLZ4-micelles**

- Targeting PLZ4-micelles deliver much more drug load to bladder cancer xenografts than nonbladder cancer xenografts in the same mice.
- Targeting micelles loaded with paclitaxel are more effective in controlling cancer growth and improving overall survival than nontargeting micelles.
- Paclitaxel formulated in micelles is less toxic than free paclitaxel, which allows the administration of three-times the maximum tolerated dose without increasing the toxicity.

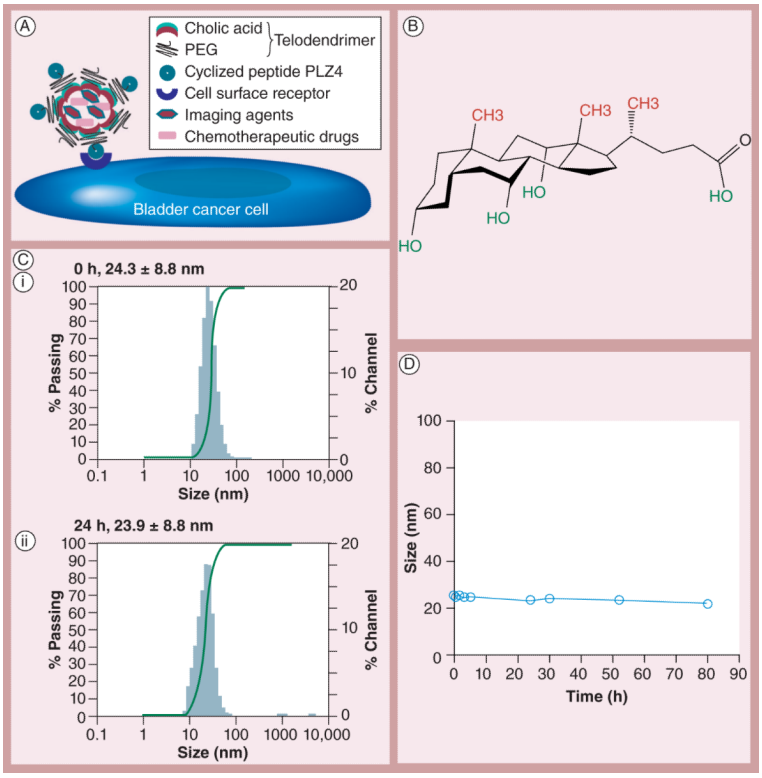

Figure 1. Characterization of PLZ4-micelles

(A) Illustration of PLZ4-micelles. Telodendrimers are composed of dendritic octamers of cholic acid conjugated at one end to PEG, and PLZ4 to the other end of PEG. Cholic acid contains a facial amphiphilic structure with hydrophobic CH_3 groups (red) at one side and hydrophilic OH groups (green) at the other. When telodendrimers self-assemble into nanometer-scale micelles, cholic acid units form the hydrophobic core of micelles that can encapsulate hydrophobic drugs such as paclitaxel, and/or imaging agents, and the hydrophilic PEG together with PLZ4 is displayed on the surface of micelles. **(B)** Structure of cholic acid. **(C)** Dynamic light scattering showing the size of PLZ4-micelles **(i)** before and **(ii)** 24 h after incubation with phosphate-buffered saline with 10% fetal bovine serum at 37°C. **(D)** Stability assay. The size of PLZ4-micelles remained stable during the 4-day incubation with phosphate-buffered saline with 10% fetal bovine serum.

PEG: Polyethylene glycol.

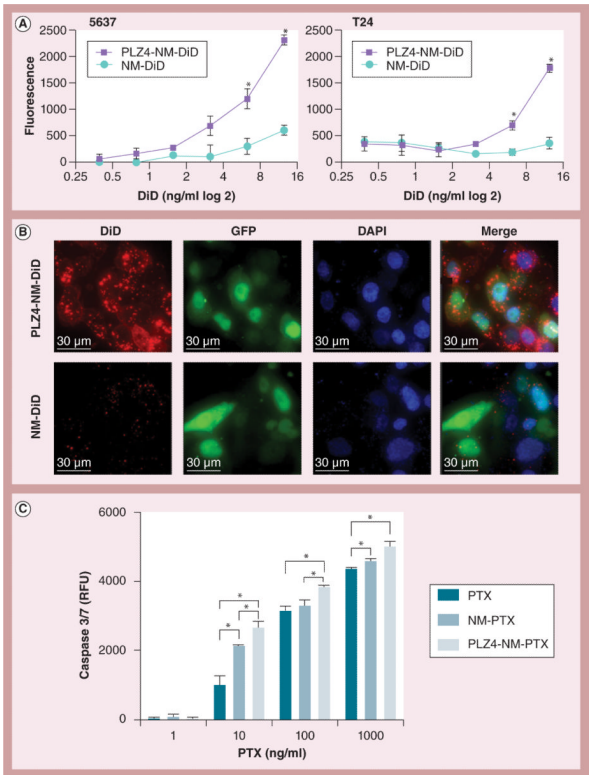

Figure 2. Targeted delivery, subcellular distribution and biological effects of targeting PLZ4-micelles

(A) Demonstrates more efficient delivery of targeting micelles to bladder cancer cells. Human bladder cancer cell lines 5637 and T24 were incubated with different concentrations of nontargeting (NM-DiD) or targeting (PLZ4-NM-DiD) micelles, both loaded with near-infrared dye DiD for 30 min. **(B)** Tomographies showing subcellular distribution of micelles in bladder cancer cell line 5637. 5637 cells expressing GFP (green fluoresce, cytoplasm/nucleus) were treated with NM-DiD or PLZ4-NM-DiD for 30 min. Cells were mounted with DAPI (blue, nucleus staining) medium for high-resolution imaging. **(C)** Dose-dependent induction of caspase 3/7. 5637 cells were treated with free PTX, PTX in nontargeting micelles (NM-PTX) or PTX in targeting micelles (PLZ4-NM-PTX) for 24 h before measurement of caspase 3/7.

*$p < 0.05$.

DAPI: 4′,6-diamidino-2-phenylindole; NM-DiD: Nanomicelle loaded with DiD; NM-PTX: Nanomicelle loaded with paclitaxel; GFP: Green fluorescence protein; PLZ4-NM-DiD: Nanomicelle coated with PLZ4 and loaded with DiD; PLZ4-NM-PTX: Nanomicelle coated with PLZ4 and loaded with paclitaxel; PTX: Paclitaxel; RFU: Relative fluorescence units.

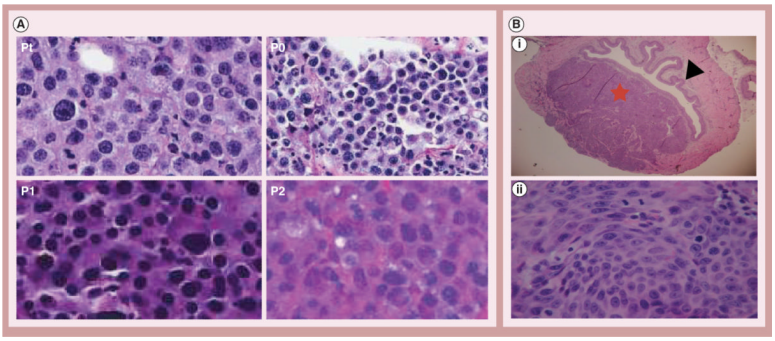

Figure 3. Patient-derived xenografts in NOD SCID-γ mice

(A) Morphological studies of patient-derived xenografts (400×), showing that the fidelity of bladder cancer cell morphology is maintained during the passaging in NOD SCID-γ mice. **(B)** Orthotopic invasive bladder cancer. Single-cell suspension was injected into the bladder wall to establish orthotopic bladder cancer models. **(B,i)** Cross-section of excised bladder showing a tumor xenograft expanded and invaded into the lamina propria and full thickness of the muscularis propria (20×). Black arrow: normal urothelial cells; red star: patient-derived xenografts in the bladder wall penetrating into the extravesical space. **(B,ii)** High magnification showing patient-derived xenografts cancer cells (400×).

Pt: Patient specimen; P0: Passage 0 (first xenograft established in NSG mice); P1: Passage 1; P2: Passage 2.

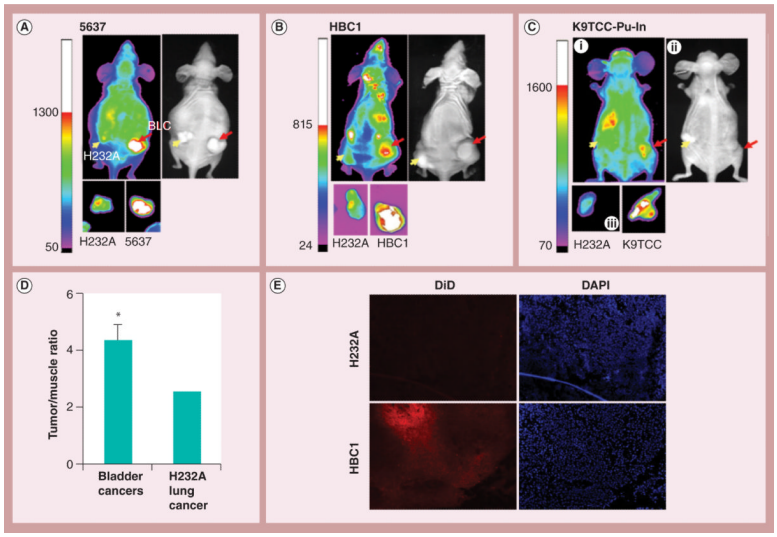

Figure 4. Comparison of targeting PLZ4-micelle delivery to lung and bladder cancer xenografts

Nude mice were injected with H232A lung cancer cells at the left flank (yellow arrows) and BLCs at the right (red arrows). Targeting PLZ4-micelles loaded with DiD were injected through the tail vein for *in vivo* and *ex vivo* imaging at 8 h after dosing. **(A)** Human cell line 5637; **(B)** patient-derived xenografts (HBC1); **(C)** dog bladder cancer cell line K9TCC-Pu-In. **(C,i)** *In vivo* imaging; **(C,ii)** light imaging; and **(C,iii)** *ex vivo* imaging. **(D)** Imaging ana lysis and statistics from three independent experiments were performed and presented. *$p < 0.05$. **(E)** Direct visualization of DiD in tumor specimens. Cryosection of HBC1 and H232A xenografts were visualized under fluorescence microscope (100×). Red color represented DiD signals, while DAPI (blue) represented nucleus location. Significantly more fluorescence was detected in HBC1 than in the H232A xenograft in the same mouse. BLC: Bladder cancer cell; DAPI: 4′,6-diamidino-2-phenylindole; HBC1: Human bladder cancer 1.

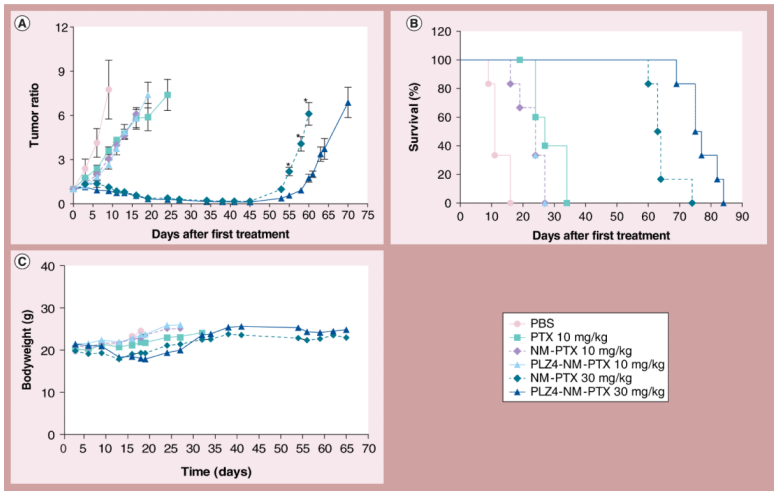

Figure 5. Therapeutic efficacy in mice carrying subcutaneous bladder cancer xenografts

(A) Control of cancer growth by different treatments. This *in vivo* therapeutic efficacy study was performed on NOD SCID-γ mice carrying subcutaneous human bladder cancer xenografts. They were treated through intravenous injection with PBS, 10 mg/kg PTX, 10 mg/kg NM-PTX or PLZ4-NM-PTX, and 30 mg/kg NM-PTX or PLZ4-NM-PTX for a total of six doses on days 0, 3, 6, 9, 13 and 16 after tumor size reached 150–200 mm^3 (n = 6 for each treatment). * $p < 0.05$ for the comparison of xenograft sizes between the mice treated with nontargeting micelles and those treated with targeting PLZ4-micelles. **(B)** Survival curve of mice in each treatment group. The difference of overall survival between nontargeting and targeting groups at 30 mg/kg was statistically significant ($p = 0.002$). **(C)** Weight change of mice in different treatment groups.

NM-PTX: Nanomicelle loaded with paclitaxel; PBS: Phosphate-buffered saline; PLZ4-NM-PTX: Nanomicelle coated with PLZ4 and loaded with paclitaxel; PTX: Paclitaxel.

Table 1

Treatment groups, median survival, blood counts and chemical panels 14 days after treatment.

Treatment	Median survival (days)	WBC (1000/ml)	RBC (million/ml)	Platelets (1000/ml)	Creatinine (mg/dl)	Total bilirubin (mg/dl)	Aspartate aminotransferase (U/l)
PBS	11	3.96 ± 1.40	8.57 ± 0.40	1030.67 ± 280.00	0.12 ± 0.01	0.19 ± 0.05	29.30 ± 12.40
PTX 10 mg/kg	27	1.16 ± 0.19	6.08 ± 0.41	1693.33 ± 125.73	0.12 ± 0.03	0.54 ± 0.17	23.50 ± 5.45
NM-PTX 10 mg/kg	24	2.29 ± 0.87 *	7.80 ± 0.38 *	1188.33 ± 119.32 *	0.14 ± 0.05	0.29 ± 0.03	23.3 ± 1.13
PLZ4-NM-PTX 10 mg/kg	24	2.03 ± 0.81 *	8.00 ± 0.43 *	1230.67 ± 307.47 *	0.11 ± 0.02	0.29 ± 0.07	23.30 ± 1.86
NM-PTX 30 mg/kg	64	1.17 ± 0.29	5.80 ± 0.60	1889.50 ± 198.66	0.13 ± 0.05	0.47 ± 0.09	24.80 ± 4.53
PLZ4-NM-PTX 30 mg/kg	76	1.08 ± 0.28	7.16 ± 0.47 *	1617.83 ± 192.43	0.14 ± 0.03	0.29 ± 0.15	17.53 ± 2.38

NM: Nanomicelle; NM-PTX: Nanomicelle loaded with PTX; PBS: Phosphate-buffered saline; PLZ4-NM-PTX: Nanomicelle coated with PLZ4 and loaded with paditaxel; PTX: Paditaxel; RBC: Red blood cell count; WBC White blood cell count.

* $p < 0.05$ when compared with the results in mice treated with free PTX 10 mg/kg.